Journal of Nuclear Medicine, published on June 14, 2019 as doi:10.2967/jnumed.119.226407

Predictive Role of Temporal Changes in Intratumoral Metabolic Heterogeneity during Palliative Chemotherapy in Patients with Advanced Pancreatic Cancer: A Prospective Cohort Study

Shin Hye Yoo[1*], Seo Young Kang[2*], Gi Jeong Cheon[2], Do-Youn Oh[1,3], Yung-Jue Bang[1,3]

[1]Department of Internal Medicine, Seoul National University Hospital;

[2]Department of Nuclear Medicine, Seoul National University Hospital;

[3]Cancer Research Institute, Seoul National University College of Medicine;

[*]These authors contributed equally to this work.

Running title: intratumoral metabolic heterogeneity

Corresponding author:

Do-Youn Oh, MD, PhD,

Department of Internal Medicine, Seoul National University Hospital,

101 Daehak-ro, Jongno-gu, Seoul 03080, Korea

Tel: +82-2-2072-0701; Fax: +82-2-762-9662

E-mail: ohdoyoun@snu.ac.kr

First author:

Shin Hye Yoo (Fellow)

Department of Internal Medicine, Seoul National University Hospital,

101 Daehak-ro, Jongno-gu, Seoul 03080, Korea

Tel: +82-2-2072-2228; Fax: +82-2-762-9662

E-mail: ifi1024@gmail.com

Seo Young Kang (Fellow)

Department of Nuclear Medicine, Seoul National University Hospital,

101 Daehak-ro, Jongno-gu, Seoul 03080, Korea

Tel: +82-2-2072-2228; Fax: +82-2-762-9662

E-mail: eironn02@gmail.com

Total manuscript word count: 4,990

ABSTRACT

Metabolic intratumoral heterogeneity (ITH) is known to be related with cancer treatment outcome. However, information on the temporal changes in metabolic ITH during chemotherapy and the correlations between metabolic changes and treatment outcomes in patients with pancreatic cancer is sparse. We aimed to analyze the temporal changes in metabolic ITH and the predictive role of its changes in advanced pancreatic cancer patients who underwent palliative chemotherapy.

Methods: We prospectively enrolled unresectable locally advanced or metastatic pancreatic cancer patients before first-line palliative chemotherapy. [^{18}F]fluorodeoxyglucose positron emission tomography was performed at baseline (T1) and at the first response follow-up (T2). Standardized uptake values (SUVs), volumetric parameters, and textural features of the primary pancreatic tumor were analyzed. Relationships between the parameters at T1, T2, and changes in the parameters with treatment response, progression-free survival (PFS), and overall survival (OS) were assessed.

Results: Among 63 enrolled patients, the best objective response rate was 25.8% (95% confidence interval [CI], 14.6% to 37.0%). The median PFS and OS were 7.1 months (95% CI, 5.1 to 9.7 months) and 10.1 months (95% CI, 8.6 to 12.7 months), respectively. Most of the parameters changed significantly during the first-line chemotherapy, in a way of reducing ITH. Metabolic ITH was more profoundly reduced in responders than in nonresponders. Multiple Cox regression analysis identified high baseline compacity (P=0.023) and smaller decreases in SUV_{peak} (P=0.007) and $entropy_{gray\text{-}level\ co\text{-}occurrence\ matrix\ (GLCM)}$ (P=0.033) to be independently associated with poor PFS. Patients with a high CA 19-9 (P=0.042), high pretreatment SUV_{peak} (P=0.008), and high coefficient of variance at T2 (P=0.04) showed worse OS.

Conclusions: Reduction in metabolic ITH during palliative chemotherapy in advanced pancreatic cancer patients is associated with treatment response and might be predictive of PFS and OS.

Keywords: [^{18}F]FDG PET; intratumoral heterogeneity; tumor metabolism; pancreatic cancer; texture analysis;

INTRODUCTION

Malignant tumors contain subsets of cancer cells that present different levels of cellular proliferation, invasiveness, metastatic potential, and susceptibilities to anticancer drugs, and show complicated cell-cell interactions. This intratumoral heterogeneity (ITH) has been found to be clinically important with regard to patient outcome and response to therapy, resulting in growing interest in this area of research. ITH is most commonly thought to be the result of subclonal genetic diversity, which leads to variations in stromal architecture, oxygen consumption, and glucose metabolism (*1*).

To evaluate ITH in a non-invasive manner, various imaging modalities can be used for depicting ITH by combining data from three-dimensional elements called voxels (*1,2*). Computed tomography (CT) or magnetic resonance imaging has benefits to aid diagnosis, characterization and response assessment of tumors using ITH. [^{18}F]fluoro-2-deoxy-d-glucose (FDG) positron emission tomography/CT (PET/CT), which quantifies tumor metabolic activity, is also a useful imaging modality for diagnosis, follow-up assessment, and response to treatment. With regard to regional variations in glucose metabolism, ITH can be evaluated by [^{18}F]FDG PET/CT. Studies on metabolic ITH suggest that it might affect the outcomes and responses to treatment of patients with several types of malignancies (*3-6*).

Patients with unresectable or metastatic pancreatic cancer have a major disease burden and show high mortality and poor response to treatment (*7*). Pancreatic cancer is a stroma-rich tumor that usually shows an elevated level of ITH (*8*). As obtaining sufficient tissue for identifying ITH histopathologically is usually difficult, evaluating metabolic ITH in pancreatic cancer patients with imaging modalities is reasonable alternative. There are a few retrospective studies (9-11) that have investigated the predictive role of metabolic ITH in pancreatic cancer. However, the

studies address heterogeneous patient groups, raising questions about the reliability of the results of the study. In addition, whether a change in metabolic ITH after chemotherapy is associated with response to treatment and outcome of patients or not still remains unclear.

We aimed to analyze the temporal changes in metabolic ITH and the predictive role of delta-radiomics in a prospective cohort of patients with unresectable or metastatic pancreatic cancer who underwent palliative chemotherapy.

MATERIALS AND METHODS

Patients and Data Collection

We prospectively enrolled patients with advanced gastric cancer, pancreatic cancer, or biliary tract cancer beginning in October 2013. The inclusion criteria were as follows: 1) histopathologically confirmed advanced cancer; 2) unresectable, locally advanced, or metastatic cancer; 3) planned palliative chemotherapy (chemotherapy-naïve); and 4) signed informed consent. For this analysis, we included pancreatic cancer patients only. Cases of primary pancreatic tumor that could not be examined were excluded (Supplemental Fig. 1). Demographic and clinical information including carcinoembryonic antigen level and carbohydrate antigen 19-9 (CA 19-9) level were collected. Response to chemotherapy was assessed by the Response Evaluation Criteria in Solid Tumors (RECIST) guideline, version 1.1 (*12*), which were applied to both primary and metastatic lesions. [^{18}F]FDG PET/CT was performed before the initiation of palliative chemotherapy (T1) and at the time of the first evaluation of response (T2), usually after 2 or 3 cycles of chemotherapy for all participants, and then serially performed for each evaluation of response, when possible. The study protocol was reviewed and approved by the institutional review board of the Seoul National University Hospital (no. H-1307-132-508). We

conducted the study in accordance with the Principles of the Declaration of Helsinki. Informed consent was obtained from all individual participants included in the study.

18-F-FDG PET/CT Protocol

All patients administered intravenously [^{18}F]FDG of 5.18 MBq/kg after at least six hours fasting. Serum glucose levels were less than 150 mg/dL at the time of FDG administration. [^{18}F]FDG PET/CT using dedicated PET/CT scanner (Biograph 40 True-point, Siemens, Knoxville, TN, USA) was performed at 60 min after the injection. After low-dose CT scan for attenuation correction (120 kV, 3.75 mm slice thickness), consecutive emission scan was acquired in three-dimensional (5–6 bed positions, 2.5 min/bed, 21.6-cm increments). PET images were reconstructed onto a matrix of 128×128 using the three-dimensional ordered-subsets expectation maximization algorithm (2 iterations, 21 subsets). Details on the [^{18}F]FDG PET/CT procedure have been described in our previous reports (*13,14*).

Analysis of Standardized Uptake Value (SUV) and Texture Analysis (TA)

A nuclear medicine specialist performed tumor delineation, metabolic parameter and TA without any clinical information. PET Edge, a gradient-based delineation tool in MIM (MIMVista software, version 4.1; MIM Software Inc.; Cleveland, OH, USA), was used for tumor segmentation. The volume of interest (VOI) of the primary pancreatic lesion was automatically defined. Metastatic lesions were not used in the analysis. SUV parameters including the mean SUV (SUV_{mean}), maximum SUV (SUV_{max}), and peak SUV (SUV_{peak}); and volumetric parameters including metabolic tumor volume (MTV) and total lesion glycolysis (TLG) were extracted from the VOI. The coefficient of variance (CoV), which is defined as the

standard deviation (Sd) of SUVs divided by the SUV_{mean} was calculated from the extracted parameters. The CoV is positively correlated with degree of heterogeneity in the VOI (*6*).

For TA, [^{18}F]FDG PET/CT images and delineation data were imported to LifeX Software (version 4.0), which is a multiplatform and easy-to-use freeware (*15*). Each [^{18}F]FDG PET/CT image was resampled into a 64-level gray-scale by a fixed-bin-width method with 0.3-SUV-unit scaling, from minimum to maximum SUV values of 0 to 20. We included the histogram indices and shape indices as first-order parameters, indices for the GLCM as second-order parameters, and the neighborhood gray-level different matrix (NGLDM) as higher order parameters (*16*). Definitions and explanations of the parameters derived from TA are described in Supplemental Table 1. Histogram indices provide information derived from global histogram analysis. GLCM takes into account the arrangements of pairs of voxels to extract textural indices. NGLDM corresponds to the difference in the grey-level of a single voxel and its 26 neighbors in 3 dimensions. Fig. 1 depicts a representative image of changes in metabolic ITH.

Statistical Analysis

Based on previous studies (*9,17*), sample size calculation indicated that at least 61 participants were needed (confidence interval of 95%; type II error rate of 20%) to reach an assumed relative hazard of 2.5 and a censoring rate of 30%, accounting for a drop-out rate at T2 of 5-10%.

Differences between the T1 and T2 parameters of SUV and TA were assessed by the paired t-test (for parametric analysis) or Wilcoxon signed rank test (for non-parametric analysis). We divided patients according to RECIST response to chemotherapy into 2 groups: responders (complete response [CR] or partial response [PR]) and nonresponders (stable disease [SD] or progressive disease [PD]). The Student t-test or Mann-Whitney test were used for comparing

variables of responders with those of nonresponders, after testing for normality by the Shapiro-Wilks test.

The predictive performances of SUV and TA parameters were investigated by time-dependent receiver operating characteristics (ROC) curves for progression-free survival (PFS) and overall survival (OS). PFS was defined as the time from initiation of first-line chemotherapy to the date of disease progression or death. OS was calculated from the time from initiation of first-line chemotherapy to the date of death or last follow-up. The area under the ROC curve (AUC) was calculated by the 'survivalROC' package in R open-source statistical software (R Foundation, Vienna, Austria). We dichotomized each variable as high or low, with different cut-off points that maximized the AUC. Univariate Cox proportional hazard regression analysis was performed to investigate the associations of clinical variables and SUV and TA parameters with PFS and OS. Because of the large number of SUV and TA parameters, we only included variables with AUC values>0.6 in the univariate analysis. After omission of the variables with multicollinearity, backward-selected multivariable Cox regression analyses were conducted for the significant variables with $P<0.05$ as identified by univariate analysis. Survival estimates were determined by the Kaplan-Meier method and were compared by the log-rank test. Two-sided P-values<0.05 were considered statistically significant. All statistical tests were two-sided and were performed using STATA, version 12 software (StataCorp LP, College Station, TX, USA) and R software.

RESULTS

Patients and Baseline Characteristics

With May 2018 as the cut-off date for data, a total of 63 patients were enrolled in the study (Supplemental Fig. 1). For analyses comparing T1 and T2, we excluded 2 patients who did not

undergo follow-up PET-CT scans and 1 patient whose VOI at T2 could not be obtained.

Patients' baseline characteristics are listed in Supplemental Table 2. Among 62 patients who were evaluable for tumor response to chemotherapy, 16 patients had PR and were classified as responders and 46 were classified as nonresponders (39 SD and 7 PD). The best objective response rate was 25.8% (95% confidence interval [CI], 14.6% to 37.0%), and the disease control rate was 88.7% (95% CI, 80.6% to 96.8%). During the median duration of follow-up of 11.2 months, 55 (88.7%) patients progressed and died. The median PFS was 7.1 months (95% CI, 5.1 to 9.7 months). The median OS was 10.1 months (95% CI, 8.6 to 12.7 months).

Distributions of SUV and TA Parameters at T1 and T2, and Their Changes During First-line Chemotherapy

The SUVs and TA parameters at T1 and T2, and changes in values between T1 and T2 are shown in Supplemental Table 3 and Supplemental Fig. 2. Except for skewness, kurtosis, sphericity, and $contrast_{GLCM}$, significant changes between T1 and T2 occurred for most variables. Overall, the values of all metabolic ITH parameters except busyness were found to decrease with chemotherapy.

Parameters of Responders versus Nonresponders

Table 1 compares the SUV and TA parameters of responders with those of nonresponders. At T1, the values of skewness and kurtosis in responders were significantly higher than the values in nonresponders, whereas the value for coarseness was significantly lower in responders than in nonresponders (Supplemental Fig. 3). At T2, no differences were observed between any of the variables assessed for the 2 groups. The percent change of several parameters, including most of conventional indices and some of textural indices, between T1 and T2, were significantly

associated with response. The metabolic parameters such as SUV_{peak} (P=0.007), TLG (P=0.0003), CoV (P=0.029), and MTV (P=0.0001) decreased to a greater degree in responders than in nonresponders. $Entropy_{histo}$ (P=0.043), compacity (P=0.0005), dissimilarity (P=0.022), and coarseness (P=0.0006) also decreased more in responders than in nonresponders. The value for energy increased 2-fold in responders over the value in nonresponders (P=0.019). Since energy indicates the uniformity of grey-level voxel pairs, an increased value indicates a decrease in metabolic ITH. Fig. 2 shows the decreased metabolic ITH in responders compared with nonresponders.

PFS and OS as Predicted by Clinical Variables and SUV and TA Parameters

The optimal cut-off values and corresponding AUC values for PFS and OS are listed in Supplemental Table 4. By univariate Cox regression analysis, patients with a high level of CA 19-9 and nonresponders had shorter PFS than those with lower CA 19-9 levels and responders. Significant predictors for PFS among metabolic parameters were listed in Supplemental Table 5. After omission of variables with multicollinearity, the final model for PFS showed that high pretreatment compacity (hazard ratio (HR) 2.8; 95% CI, 1.15-6.83; P=0.023), a reduction in SUV_{peak} less than 15.45% (HR 2.46; 95% CI 1.28-4.71; P=0.007), $entropy_{GLCM}$ lower than 26.12% (HR 2.54; 95% CI, 1.08-6.00; P=0.033), and being a nonresponder (HR 3.29; 95% CI, 1.54-7.01; P=0.02) were independently associated with poor PFS (Table 2; Fig. 3).

An increased pretreatment CA 19-9 level was a significantly poor prognostic factor for OS. Increased SUV_{peak}, compacity, and dissimilarity at T1 were associated with shorter OS. At T2, OS was shorter in patients with high SUV_{max}, TLG, CoV, $entropy_{histo}$, compacity, $entropy_{GLCM}$, dissimilarity, and coarseness (Supplemental Table 5). None of the change parameters with an

AUC < 0.6 were included in the univariate analysis for OS. By multivariable Cox regression analysis, an increased CA 19-9 level (HR 1.79; 95% CI, 1.02-3.14; P=0.042), being a nonresponder (HR 2.11; 95% CI, 1.08-4.15; P=0.02), high pretreatment SUV_{peak} (HR 3.31; 95% CI, 1.37-8.00; P=0.008), and high CoV at T2 (HR 2.02; 95% CI, 1.03-3.94; P=0.04) were associated with shorter OS (Table 2; Fig. 4).

DISCUSSION

Previous studies that have had limitations in study design (*9,10*) have investigated the temporal changes in metabolic ITH and the predictive role of changes in metabolic ITH for survival in patients with advanced pancreatic cancer. We demonstrated that metabolic ITH decreased during palliative chemotherapy to a greater degree in responders than in nonresponders. To our knowledge, this is the first report to demonstrate prospectively the negative changes in ITH over time in patients with advanced pancreatic cancer who were treated with systemic chemotherapy. Furthermore, we found that a less reduction of heterogeneity represented as $entropy_{GLCM}$ during a response assessment period was associated with shortened survival. These findings suggest that in addition to the clinical features of patients with pancreatic cancer, metabolic features of the tumor that are revealed on imaging can predict survival outcomes (*9,10,18*).

SUVs and most TA parameters were significantly reduced with decreasing metabolic ITH over the course of chemotherapy in our analysis, whereas only 3 parameters, SUV_{mean}, SUV_{max}, and first-order entropy decreased in lung cancer patients treated with erlotinib (*17*). Negative trends over time related to treatment have also been described for patients with other types of tumors (*3,17,18*). These findings support the hypothesis that tumor clones were initially heterogeneous and then, as a result of treatment, the predominant subclones disappeared and tumor

heterogeneity decreased (*8,19*).

Greater reductions in metabolic uptake and heterogeneity in the tumors of responders than in the tumors of nonresponders have also been found in other studies, although those studies evaluated localized chemoradiation therapy (*3,18,20*) or neoadjuvant therapy (*5*). In addition to the previously reported improvements in SUV (*14,17*) and TLG (*20,21*) during treatment, our findings indicate that the grey-level distributions in the tumor become less random and more unified than seen at baseline, and the variations in grey-level voxel pairs become minimized. This finding might indicate that an early metabolic response and change in tumor composition precedes tumor regression (*22*).

The reduction in metabolic parameters was also shown to be a significant predictor of PFS. Our findings that the percent changes in SUV_{peak} and $entropy_{GLCM}$ were significantly associated with PFS are consistent with other study results (*5,10,23-25*). An increasing reduction in randomness in grey-level voxel pairs is associated with a lengthening PFS. While the performance capacity of TA parameters was found in some studies to be superior to that of SUV parameters (*5*), we found that both SUV and TA parameters predicted PFS, and incorporated the best response in the multivariable model. We also showed that highly compact VOI was associated with poor PFS. Despite its clinical significance in our study, whether or not metabolic compacity is related to such biological characteristics as tumor density and cellularity has been unclear. Further investigation is warranted to explore such relationships.

We found that both pretreatment CA 19-9 level and SUV_{peak} were important prognostic factors for OS compared with TA-based parameters. The baseline CA 19-9 level is a well-known independent prognostic factor in pancreatic cancer patients (*9*). Although pretreatment SUV_{peak} is a poor prognostic factor for OS (*25*), the final model for OS from two studies in pancreatic

cancer patients did not include it (*9,10*). More heterogeneous study population and different treatment modalities from our study might account for discrepancies. Interestingly, we saw a negative prognostic role for an elevated CoV at T2. A high CoV represents a high degree of heterogeneity; therefore, it might be obvious that a CoV value that remains elevated at the first assessment might be a predictor of poor outcome.

This study has limitations. First, a small number of patients were involved in this study. Larger study cohorts might be needed to confirm our findings. Second, we only evaluated metabolic ITH of the primary pancreatic lesion, which might not represent the overall metabolic heterogeneity that represents every tumor lesion in patients with metastatic lesions (*18*). Third, the heterogeneity of the chemotherapy regimens that our patients received might have confounding effects. However, treatment variable was insignificant in univariate analyses, and we included it for adjustment in the multivariable models. Finally, this study contains only the training step because of limited numbers of participants. The validation step is needed using further cohort data (internal) or independent data (external).

Despite the several limitations, examining the association of metabolic ITH with treatment outcomes in patients receiving palliative chemotherapy is warranted. Our study enhances the significance of metabolic ITH in patients with advanced pancreatic cancer. Although a consensus on the best methodology for assessing metabolic ITH has not yet been achieved, we performed a comprehensive analysis of classical and textural parameters. Finally, we focused on both pretreatment and posttreatment images, whereas most studies only focused on analysis of pretreatment one (*9*). In addition, early delta-radiomics features in metabolic ITH were good predictors in PFS. In clinical perspectives, it should be very cautious to draw a conclusion that TA parameters can be used for treatment decision-making such as discontinuation of palliative

chemotherapy. However, we suggest that TA parameters can be helpful to predictive treatment outcomes rather than they are important to determine the discontinuation of treatment.

CONCLUSION

Our study demonstrated that the level of metabolic ITH reduces during palliative chemotherapy in patients with advanced pancreatic cancer, and that metabolic ITH is associated with response to therapy and is predictive of PFS and OS.

Funding

This research was supported by the Seoul National University Hospital Research Fund (grant number: 25-2014-0140) and a grant from the SNU Invitation Program for Distinguished Scholar to Dr. Do-Youn Oh. The research was also partly supported by a 2018 Seoul National University Research Grant (grant number: 800-20180367) and a grant to Dr. Gi Jeong Cheon from the Korea Health Technology R&D Project through the Korea Health Industry Development Institute (KHIDI), which is funded by the Ministry of Health & Welfare, Republic of Korea (grant number: HI14C1072).

Conflict of interest disclosure: The authors declare no potential conflicts of interest.

KEY POINTS

QUESTION: Is the temporal change of metabolic intratumoral heterogeneity during palliative chemotherapy associated with treatment outcomes in advanced pancreatic cancer patients?

PERTINENT FINDINGS: In a prospectively cohort study of 63 advanced pancreatic cancer patients, we found that metabolic intratumoral heterogeneity decreased during palliative chemotherapy to a greater degree in responders than in nonresponders. In addition to the clinical variables, a decreased reduction in heterogeneity was associated with shortened progression-free survival and overall survival in advanced pancreatic cancer patients.

IMPLICATIONS FOR PATIENT CARE: Measurements of early change of metabolic intratumoral heterogeneity during palliative chemotherapy could be imaging biomarkers to predict survival outcomes.

REFERENCES

1. O'Connor JP, Rose CJ, Waterton JC, Carano RA, Parker GJ, Jackson A. Imaging intratumor heterogeneity: role in therapy response, resistance, and clinical outcome. *Clin Cancer Res.* 2015;21:249-257.

2. Davnall F, Yip CS, Ljungqvist G, et al. Assessment of tumor heterogeneity: an emerging imaging tool for clinical practice? *Insights Imaging.* 2012;3:573-589.

3. Yang F, Thomas MA, Dehdashti F, Grigsby PW. Temporal analysis of intratumoral metabolic heterogeneity characterized by textural features in cervical cancer. *Eur J Nucl Med Mol Imaging.* 2013;40:716-727.

4. Kang SR, Song HC, Byun BH, et al. Intratumoral metabolic heterogeneity for prediction of disease progression after concurrent chemoradiotherapy in patients with inoperable stage III non-small-cell lung cancer. *Nucl Med Mol Imaging.* 2014;48:16-25.

5. Yip SS, Coroller TP, Sanford NN, Mamon H, Aerts HJ, Berbeco RI. Relationship between the temporal changes in positron-emission-tomography-imaging-based textural features and pathologic response and survival in esophageal cancer patients. *Front Oncol.* 2016;6:72.

6. Bundschuh RA, Dinges J, Neumann L, et al. Textural parameters of tumor heterogeneity in 18F-FDG PET/CT for therapy response assessment and prognosis in patients with locally advanced rectal cancer. *J Nucl Med.* 2014;55:891-897.

7. Stathis A, Moore MJ. Advanced pancreatic carcinoma: current treatment and future challenges. *Nat Rev Clin Oncol.* 2010;7:163-172.

8. Cros J, Raffenne J, Couvelard A, Pote N. Tumor heterogeneity in pancreatic adenocarcinoma. *Pathobiology.* 2018;85:64-71.

9. Hyun SH, Kim HS, Choi SH, et al. Intratumoral heterogeneity of (18)F-FDG uptake predicts survival in patients with pancreatic ductal adenocarcinoma. *Eur J Nucl Med Mol Imaging.* 2016;43:1461-1468.

10. Yue Y, Osipov A, Fraass B, et al. Identifying prognostic intratumor heterogeneity using pre- and post-radiotherapy 18F-FDG PET images for pancreatic cancer patients. *J Gastrointest Oncol.* 2017;8:127-138.

11. Cui Y, Song J, Pollom E, et al. Quantitative analysis of (18)F-fluorodeoxyglucose positron emission tomography identifies novel prognostic imaging biomarkers in locally advanced pancreatic cancer patients treated with stereotactic body radiation therapy. *Int J Radiat Oncol Biol Phys.* 2016;96:102-109.

12. Eisenhauer EA, Therasse P, Bogaerts J, et al. New response evaluation criteria in solid tumours: revised RECIST guideline (version 1.1). *Eur J Cancer.* 2009;45:228-247.

13. Park S, Ha S, Kwon HW, et al. Prospective evaluation of changes in tumor size and tumor metabolism in patients with advanced gastric cancer undergoing chemotherapy: association and clinical implication. *J Nucl Med.* 2017;58:899-904.

14. Jo J, Kwon HW, Park S, Oh DY, Cheon GJ, Bang YJ. Prospective evaluation of the clinical implications of the tumor metabolism and chemotherapy-related changes in advanced biliary tract cancer. *J Nucl Med.* 2017;58:1255-1261.

15. Nioche C, Orlhac F, Boughdad S, et al. LIFEx: a freeware for radiomic feature calculation in multimodality imaging to accelerate advances in the characterization of tumor heterogeneity. *Cancer Res.* 2018;78:4786-4789.

16. Bashir U, Siddique MM, McLean E, Goh V, Cook GJ. Imaging heterogeneity in lung cancer: techniques, applications, and challenges. *AJR Am J Roentgenol.* 2016;207:534-543.

17. Cook GJ, O'Brien ME, Siddique M, et al. Non-small cell lung cancer treated with erlotinib: heterogeneity of (18)F-FDG uptake at PET-association with treatment response and prognosis. *Radiology.* 2015;276:883-893.

18. Dong X, Sun X, Sun L, et al. Early change in metabolic tumor heterogeneity during chemoradiotherapy and its prognostic value for patients with locally advanced non-small cell lung cancer. *PLoS One.* 2016;11:e0157836.

19. Heeschen C, Sancho P. More challenges ahead-metabolic heterogeneity of pancreatic cancer stem cells. *Mol Cell Oncol.* 2016;3:e1105353.

20. Usmanij EA, de Geus-Oei LF, Troost EG, et al. 18F-FDG PET early response evaluation of locally advanced non-small cell lung cancer treated with concomitant chemoradiotherapy. *J Nucl Med.* 2013;54:1528-1534.

21. van Helden EJ, Vacher YJL, van Wieringen WN, et al. Radiomics analysis of pre-treatment [(18)F]FDG PET/CT for patients with metastatic colorectal cancer undergoing palliative systemic treatment. *Eur J Nucl Med Mol Imaging.* 2018;45:2307-2317.

22. Van den Abbeele AD. The lessons of GIST--PET and PET/CT: a new paradigm for imaging. *Oncologist.* 2008;13 Suppl 2:8-13.

23. Park S, Ha S, Lee SH, et al. Intratumoral heterogeneity characterized by pretreatment PET in non-small cell lung cancer patients predicts progression-free survival on EGFR tyrosine kinase inhibitor. *PLoS One.* 2018;13:e0189766.

24. Wu J, Aguilera T, Shultz D, et al. Early-stage non-small cell lung cancer: quantitative imaging characteristics of (18)F-fluorodeoxyglucose PET/CT allow prediction of distant metastasis. *Radiology.* 2016;281:270-278.

25. Vanderhoek M, Perlman SB, Jeraj R. Impact of the definition of peak standardized uptake value on quantification of treatment response. *J Nucl Med.* 2012;53:4-11.

Figure Legends

Fig. 1 A representative image showing metabolic ITH changes from [^{18}F]FDG PET/CT images at T1 (upper) and T2 (lower) in a 61-year-old male patient. The histogram and AUC-CSH show decreased metabolic ITH after palliative chemotherapy.

[^{18}F]FDG PET/CT = [18F]fluoro-2-deoxy-d-glucose positron emission tomography/computed tomography; AUC-CSH = area under the curve of the cumulative SUV volume histogram; ITH = intratumoral heterogeneity; ROI = region of interest;

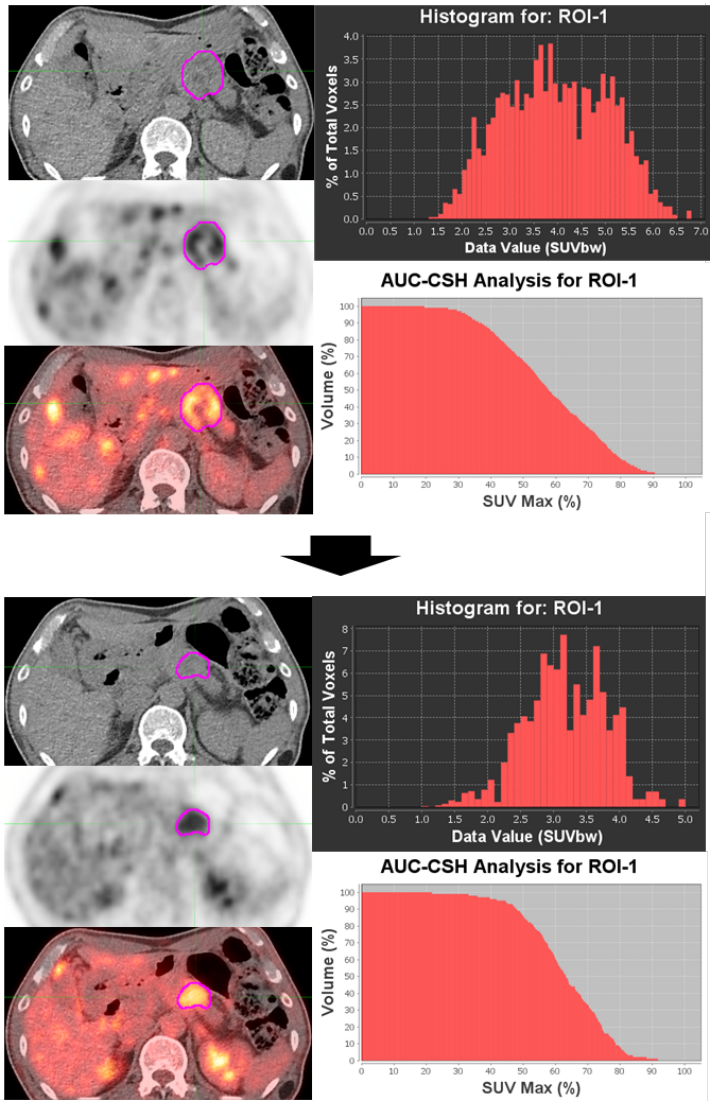

Fig. 2 Percent changes in metabolic parameters in relation to best response: SUV_{peak} (A), TLG (B), CoV (C), compacity (D), energy (E), dissimilarity (F), coarseness (G). SUV = standardized uptake value; TLG = total lesion glycolysis; CoV = coefficient of variance;

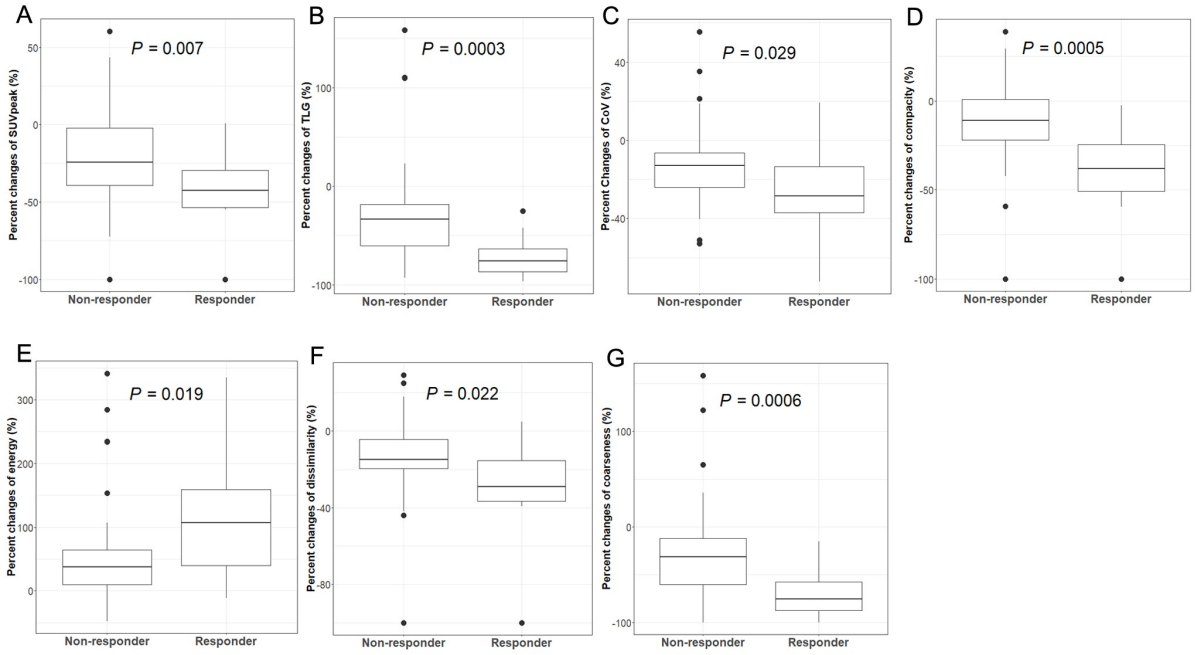

Fig. 3 Kaplan-Meier survival curves for progression-free survival according to compacity at T1 (A), percent change in SUV_{peak} (B), and percent change in $entropy_{GLCM}$ (C). SUV = standardized uptake value; GLCM = gray-level co-occurrence matrix;

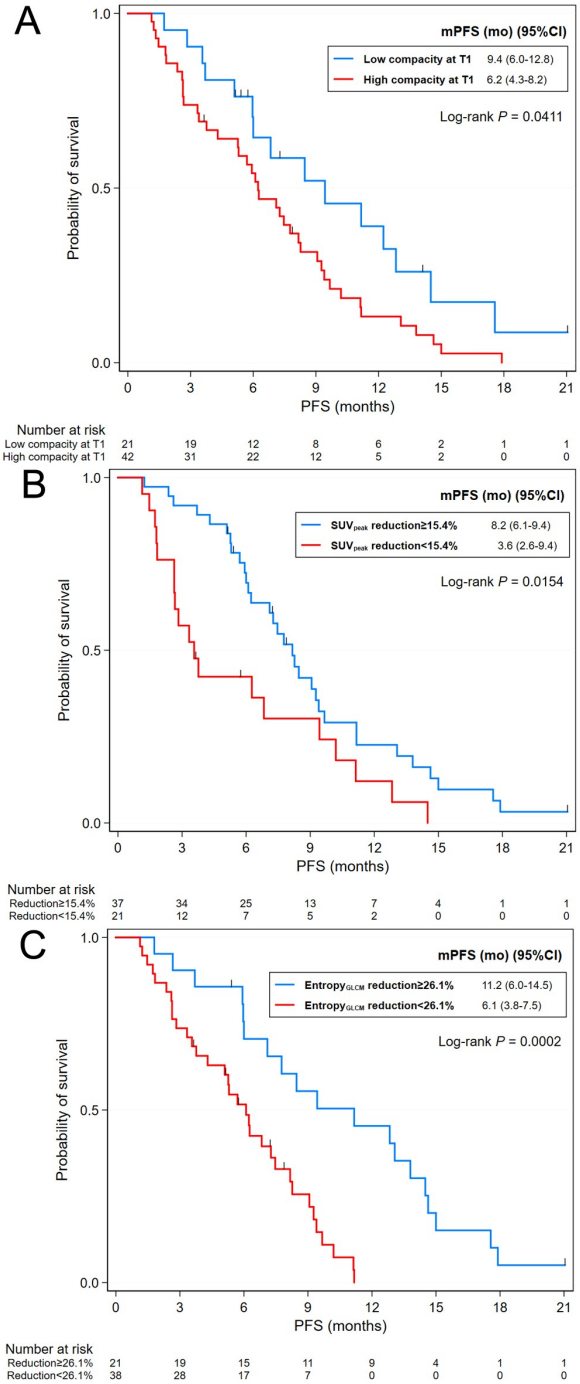

Fig. 4 Kaplan-Meier survival curves for overall survival according to SUV_{peak} at T1 (A), CoV at T1 (B), and baseline CA 19-9 level (C). SUV = standardized uptake value; CoV = coefficient of variance; CA 19-9 = carbohydrate antigen 19-9;

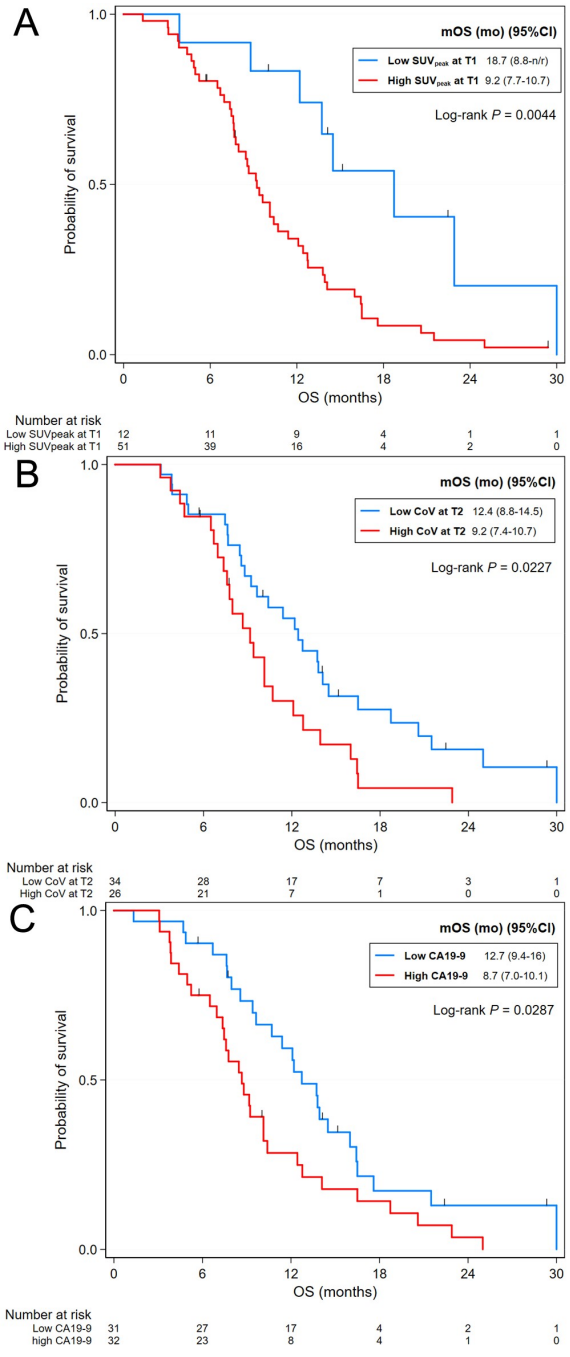

Table 1. Comparison of parameters between responders and non-responders

Parameter	T1 (baseline) (*N*=63)			T2 (first assessment) (*N*=60)			Percent change* (*N*=60)		
	Non-responder *N*=46 (74.2%)	Responder *N*=16 (25.8%)		Non-responder *N*=46 (74.2%)	Responder *N*=16 (25.8%)		Non-responder *N*=46 (74.2%)	Responder *N*=16 (25.8%)	
	Mean (Sd)		*P*	Mean (Sd)		*P*	Mean (Sd)		*P*
Conventional Indices									
SUV_{max}	8.51 (0.51)	9.13 (0.81)	0.52	6.44 (2.72)	6.09 (2.75)	0.739	-18.73 (4.53)	-31.94 (5.85)	0.128
SUV_{peak}	6.98 (3.29)	7.72 (2.73)	0.394	5.11 (2.51)	4.25 (3.06)	0.283	-22.89 (31.23)	-47.19 (32.00)	0.007
TLG	158.90 (204.55)	231.05 (226.52)	0.085	95.92 (134.86)	66.51 (68.97)	0.318	-22.56 (51.07)	-72.19 (20.52)	0.0003
CoV	0.27 (0.14)	0.28 (0.07)	0.204	0.23 (0.11)	0.20 (0.06)	0.447	-12.45 (20.87)	-26.62 (22.02)	0.029
MTV	37.59 (55.56)	46.6 (37.04)	0.077	28.99 (50.53)	17.47 (17.03)	0.447	-17.36 (48.35)	-65.64 (23.23)	0.0001
Histogram Indices									
Skewness	0.5 (0.4)	0.3 (0.4)	0.016	0.42 (0.38)	0.33 (0.33)	0.417	10.03 (171.29)	105.63 (344.67)	0.545
Kurtosis	3.0 (1.3)	2.7 (0.7)	0.048	2.98 (0.84)	2.73 (0.39)	0.37	3.50 (23.57)	4.56 (15.39)	0.872
Entropy $_{(log2)}$	3.7 (0.6)	4.0 (0.5)	0.144	3.23 (0.77)	3.09 (0.82)	0.56	-12.77 (17.02)	-23.22 (16.71)	0.043
Energy	0.10 (0.04)	0.07 (0.03)	0.172	0.14 (0.08)	0.16 (0.09)	0.591	54.89 (80.49)	112.55 (96.27)	0.019
Shape Indices									
Sphericity	0.99 (0.16)	0.95 (0.26)	0.515	0.94 (0.30)	0.81 (0.42)	0.242	-5.59 (26.35)	-19.55 (41.74)	0.389
Compacity	1.7 (0.7)	1.9 (0.7)	0.063	1.45 (0.73)	1.19 (0.74)	0.427	-15.02 (30.21)	-44.58 (31.80)	0.0005
GLCM									
Contrast	0.41 (0.09)	0.39 (0.08)	0.436	0.43 (0.16)	0.38 (0.22)	0.62	8.16 (35.71)	-3.09 (54.03)	0.783
Correlation	0.02 (0.01)	0.01 (0.01)	0.159	0.03 (0.03)	0.03 (0.03)	0.765	114.29 (238.48)	171.28 (216.00)	0.3001
Entropy $_{(log2)}$	0.55 (0.15)	0.60 (0.13)	0.277	0.44 (0.20)	0.40 (0.25)	0.713	-14.08 (54.67)	-33.26 (45.40)	0.183
Dissimilarity	2.02 (0.33)	2.17 (0.25)	0.118	1.65 (0.64)	1.41 (0.81)	0.301	-17.09 (27.48)	-36.68 (35.00)	0.022
NGLDM									
Coarseness	524.33 (643.33)	704.76 (518.63)	0.026	342.81 (487.42)	222.71 (227.81)	0.334	-28.55 (51.36)	-71.44 (24.14)	0.0006
Contrast	0.89 (0.05	0.90 (0.04)	0.885	0.79 (0.26)	0.69 (0.36)	0.37	-8.88 (25.71)	-22.59 (40.27)	0.123
Busyness	0.02 (0.016)	0.02 (0.011)	0.074	0.027 (0.021)	0.025 (0.023)	0.626	52.41 (143.84)	119.57 (178.80)	0.057

SUV = standardized uptake values; TLG = total lesion glycolysis; CoV = coefficient of variation; MTV = metabolic tumor volume; GLCM = gray-level co-occurrence matrix; NGLDM = neighboring gray-level dependence matrix;

*The percent change was calculated by 100 × [value at the first assessment (T2) minus the baseline value (T1)] / value at the baseline (T1)

Table 2. Multivariable Cox regression analysis for PFS and OS

	PFS				OS		
	aHR*	95% CI	*P*		aHR†	95% CI	*P*
Best response	3.29	1.54-7.01	0.002	**Best response**	2.11	1.08-4.15	0.029
Compacity at T1	2.8	1.15-6.83	0.023	**CA 19-9**	1.79	1.02-3.14	0.042
Percent change of SUV_{peak}	2.46	1.28-4.71	0.007	**SUV_{peak} at T1**	3.31	1.37-8.00	0.008
Percent change of $Entropy_{GLCM}$	2.54	1.08-6.00	0.033	**CoV at T2**	2.02	1.03-3.94	0.04

PFS = progression-free survival; OS = overall survival; SUV = standardized uptake values; CoV = coefficient of variation; CA 19-9 = carbohydrate antigen 19-9; GLCM = gray-level co-occurrence matrix; TLG = total lesion glycolysis;

*This backward-selected multivariable Cox regression model for PFS included age, gender, initial disease status, treatment, performance status by the Eastern Cooperative Oncology Group, CA 19-9, best response, variables at T1 (skewness, compacity), T2 (SUV_{max}, CoV, $Entropy_{GLCM}$, dissimilarity) and percent changes (SUV_{peak}, TLG, CoV, $Entropy_{GLCM}$)

†This backward-selected multivariable Cox regression model for OS included age, gender, initial disease status, treatment, performance status by the Eastern Cooperative Oncology Group, CA 19-9, best response, variables at T1 (SUV_{peak}, compacity) and T2 (SUV_{max}, TLG, CoV, $Entropy_{GLCM}$, and dissimilarity).

Supplemental Figure Legends

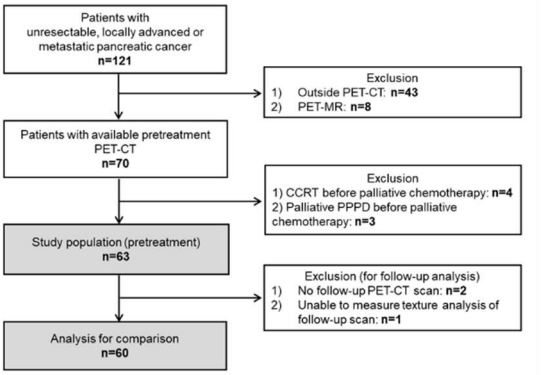

Supplemental Fig. 1 Flow chart of enrollment of study participants.

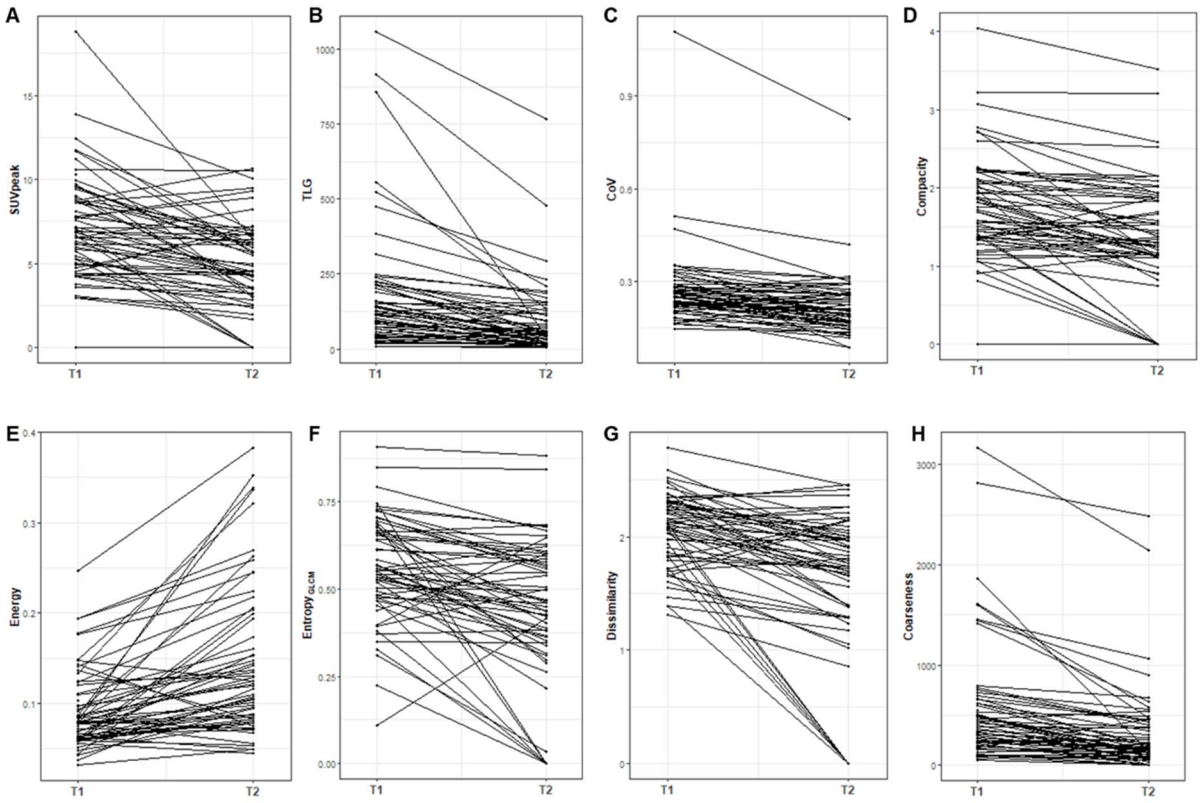

Supplemental Fig. 2 Changes in metabolic parameters between 2 time points (T1 and T2) showing individual linear plots for the following: SUVpeak (A), TLG (B), CoV (C), compacity (D), energy (E), entropy$_{GLCM}$ (F), dissimilarity (G), and coarseness (H).

SUV= standardized uptake value; TLG = total lesion glycolysis; CoV = coefficient of variance; GLCM = gray-level co-occurrence matrix;

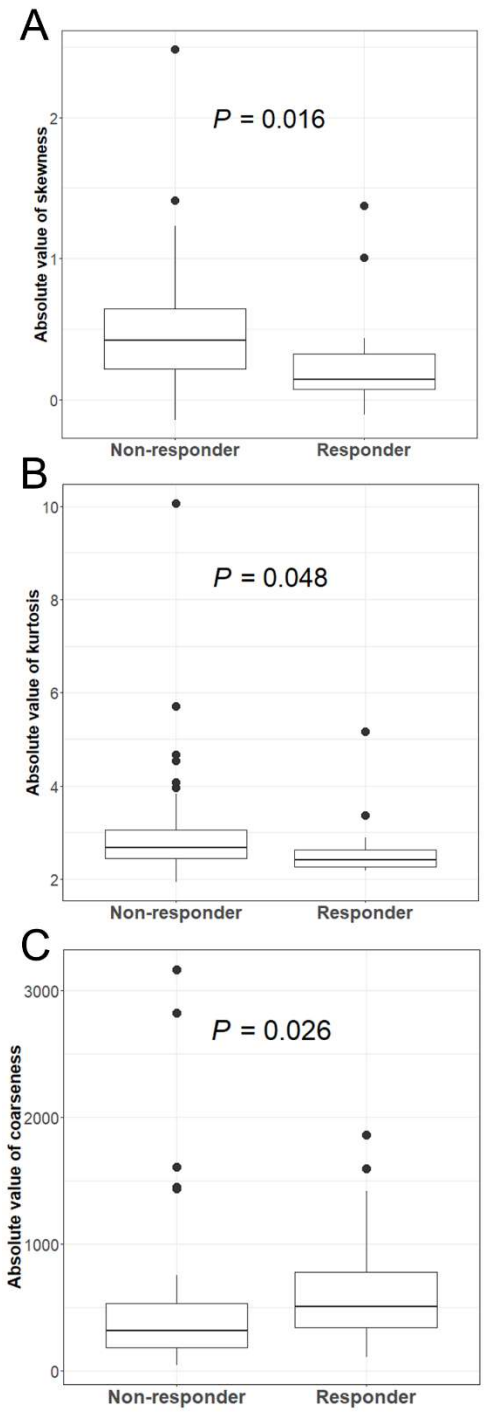

Supplemental Fig. 3 Baseline metabolic parameters in relation to best response: skewness (A), kurtosis (B), and coarseness (C).

Supplemental Table 1. Type of texture analysis parameters

Category	Parameter	Description
Histogram Indices	Skewness	measures the asymmetry of the grey-level distribution in the histogram
	Kurtosis	measures whether the grey-level distribution is peaked of flat relative to a normal distribution
	Entropy	measures the randomness of the distribution
	Energy	measures the uniformity of the distribution
Shape Indices	Sphericity	measures how spherical a volume of interest is
	Compacity	measures the degree to which the volume of interest is compact
GLCM	Correlation	linear dependency of grey-levels in GLCM
	Contrast	local variations in the GLCM
	Entropy	randomness of grey-level voxel pairs
	Dissimilarity	variation of grey-level voxel pairs
NGLDM	Coarseness	level of spatial rate of change in intensity
	Contrast	intensity difference between neighboring regions
	Busyness	spatial frequency of changes in intensity

GLCM = gray-level co-occurrence matrix; NGLDM = neighboring gray-level dependence matrix;

Supplemental Table 2. Baseline characteristics of study population (*N*=63)

Variables	*N*	%
Age (yr), median (range)	60	40-84
≥60	34	54.0
<60	29	46.0
Gender		
Male	39	61.9
Female	24	38.1
Initial disease status		
Locally advanced, unresectable	14	22.2
Metastatic	49	77.8
T stage		
T2	5	7.9
T3	18	38.6
T4	40	63.5
N stage		
N0	1	1.6
N1	20	31.7
N2	42	66.7
Comorbidity		
Hypertension	16	25.4
DM	22	34.9
ECOG performance status		
0	22	34.9
1-2	41	65.1
BMI (kg/m2), median (range)	22.2	16.1-29.7
≥25	16	25.4
20-24.9	38	60.3
<20	9	14.3
CEA (ng/mL), median (range)	4.2	0.5-12990
CA 19-9 (U/mL), median (range)	755	2-107400
WBC (x10^3/uL), median (range)	6.3	2.6-13.8

Total bilirubin (mg/dL), median (range)	0.6	0.3-2.7
Albumin (mg/dL), median (range)	4	2.8-4.9
First-line chemotherapy		
Regimen		
FOLFIRINOX	44	69.8
Gemcitabine/nab-Paclitaxel	8	12.7
Gemcitabine/Cisplatin	6	9.5
Gemcitabine/Erlotinib	2	3.2
Gemcitabine alone	3	4.8
Duration of first-line chemotherapy (mo), median (range)	5.2	0.8-29.4
Number of first-line chemotherapy cycles, median (range)	8	2-39
Dose reduction rate (%), median (range)	20	0-40
Best Response		
Partial response	16	25.4
Stable disease	39	61.9
Progressive disease	7	11.1
Not evaluable	1	1.6
Time to best response (mo), median (range)	1.7	1-7.5
Cycles till best response, median (range)	3	2-12
Progression-free survival (mo), median (95% CI)	7.1	5.1-9.7
Overall survival (mo), median (95% CI)	10.1	8.6-12.7
Follow-up duration (mo), median (range)	11.2	1.3-31.6

yr = year; ECOG = Eastern Cooperative Oncology Group; BMI = body-mass index; CEA = Carcinoembryonic antigen; CA 19-9 = carbohydrate antigen 19-9; WBC = white blood cell; FOLFIRINOX = folfirinic acid/fluorouracil/irinotecan/oxaliplatin; mo = month; CI = confidence interval;

Supplemental Table 3. Metabolic parameters at baseline (T1) and the first assessment (T2), and percent changes

Parameter	T1 (baseline) (*N*=63)				T2 (first assessment) (*N*=60)				Percent change* (*N*=60)				
	Mean	Sd	Median	Range	Mean	Sd	Median	Range	Mean	Sd	Median	Range	*P*
Conventional Indices													
SUV_{max}	8.62	3.36	8.21	3.39—20.63	6.35	2.71	6.1	2.04—12.70	-22.03	29.06	-27.71	-71.74—67.47	<0.001
SUV_{peak}	7.13	3.14	6.86	0—18.78	4.89	2.66	4.73	0—10.66	-27.69	33.24	-28.96	-100—60.50	<0.001
TLG	177.26	209.25	116.84	7.14—1058.73	88.57	121.89	49.72	4.58—765.95	-40.22	48.9	-47.16	-96.42—158.51	<0.001
CoV	0.27	0.13	0.25	0.15—1.11	0.22	0.10	0.21	0.09—0.82	-15.99	21.86	-16.54	-72.19—55.54	<0.001
MTV	40	50.88	25.65	1.71—332.75	26.12	44.71	11.64	1.16—298.89	-29.43	48.12	-35.19	-96.93—123.51	<0.001
Histogram Indices													
Skewness	0.43	0.43	0.35	-0.14—2.48	0.40	0.36	0.37	-0.24—1.77	33.93	227.62	-17.53	-370.11—1069.95	0.757
Kurtosis	2.93	1.17	2.6	1.94—10.06	2.92	0.76	2.76	1.93—6.53	3.76	21.69	3.18	-47.73—67.91	0.242
Entropy $_{(log2)}$	3.79	0.61	3.83	2.31—5.17	3.19	0.78	3.27	1.57—4.62	-15.38	17.41	-16.29	-51.53—32.32	<0.001
Energy	0.09	0.04	0.08	0.03—0.25	0.15	0.08	0.12	0.05—0.38	69.3	87.55	45.99	-47.48—341.29	<0.001
Shape Indices													
Sphericity	0.98	0.19	1.0	0—1.11	0.9	0.33	1.02	0—1.12	-9.14	31.19	-0.08	-100—18.16	0.055
Compacity	1.74	0.67	1.7	0—4.04	1.38	0.73	1.32	0—3.52	-22.53	33	-15.35	-100—38.92	<0.001
GLCM													
Contrast	0.41	0.09	0.4	0.24—0.63	0.42	0.18	0.42	0—0.72	5.25	41.01	11.9	-100—90.09	0.601
Correlation	0.015	0.013	0.01	0.002—0.074	0.027	0.033	0.015	0—0.17	128.78	232.49	79.41	-100—1157.532	<0.001
Entropy $_{(log2)}$	0.57	0.15	0.56	0.11—0.91	0.43	0.22	0.46	0—0.88	-18.96	52.77	-17.09	-100—281.39	<0.001
Dissimilarity	2.06	0.32	2.11	1.31—2.78	1.59	0.68	1.77	0—2.46	-22.07	30.49	-16.38	-100—29.33	<0.001
NGLDM													
Coarseness	569.06	610.23	399.42	49.18—3167.41	312.78	438.46	169.33	0—2486.26	-39.46	49.51	-44.51	-100—158.43	<0.001
Contrast	0.89	0.05	0.9	0.73—0.96	0.77	0.29	0.87	0—0.96	-12.36	30.29	-2.06	-100—6.90	<0.001
Busyness	0.022	0.015	0.018	0.004—0.071	0.03	0.02	0.02	0—0.09	69.48	154.68	30.37	-100—825.26	0.02

SUV = standardized uptake values; TLG = total lesion glycolysis; CoV = coefficient of variation; MTV = metabolic tumor volume; GLCM = gray-level co-occurrence matrix; NGLDM = neighboring gray-level dependence matrix;

*The percent change was calculated by 100 × [value at the first assessment (T2) minus the baseline value (T1)] / value at the baseline (T1)

Supplemental Table 4. ROC curve of Parameters

	PFS		OS	
	Cut-off value	AUC-ROC	Cut-off value	AUC-ROC
T1 (baseline)				
Conventional Indices				
SUV_{max}	5.078	0.590	7.603	0.600
SUV_{peak}	4.418	0.604	4.418	0.607
TLG	81.351	0.669	81.351	0.643
CoV	0.185	0.551	0.229	0.625
MTV	17.786	0.635	17.786	0.627
Histogram Indices				
Skewness	0.151	0.621	0.119	0.579
Kurtosis	2.614	0.627	2.562	0.620
Entropy $_{(log2)}$	3.885	0.573	3.942	0.609
Energy	0.043	0.449	0.048	0.402
Shape Indices				
Sphericity	0.971	0.632	0.956	0.552
Compacity	1.403	0.649	1.403	0.652
GLCM				
Contrast	0.332	0.43	0.246	0.44
Correlation	0.0037	0.452	0.0043	0.402
Entropy $_{(log2)}$	0.494	0.489	0.644	0.556
Dissimilarity	1.791	0.576	1.816	0.611
NGLDM				
Coarseness	297.301	0.588	297.301	0.611
Contrast	0.881	0.585	0.884	0.568
Busyness	0.047	0.397	-Inf	0.394
T2 (first assessment)				
Conventional Indices				
SUV_{max}	7.037	0.731	7.738	0.614
SUV_{peak}	5.733	0.755	4.529	0.59
TLG	48.946	0.802	69.265	0.663
CoV	0.215	0.787	0.178	0.65
MTV	8.717	0.796	25.099	0.669
Histogram Indices				
Skewness	0.552	0.579	0.348	0.521
Kurtosis	2.943	0.648	2.448	0.562
Entropy $_{(log2)}$	3.536	0.768	2.474	0.622
Energy	0.045	0.261	0.072	0.381

Shape Indices				
Sphericity	0.961	0.604	0.936	0.447
Compacity	1.14	0.817	1.171	0.659
GLCM				
Contrast	0.368	0.566	0.319	0.535
Correlation	0	0.473	0.009	0.503
Entropy $_{(log2)}$	0.365	0.842	0.498	0.673
Dissimilarity	1.768	0.782	1.289	0.609
NGLDM				
Coarseness	141.094	0.803	104.343	0.67
Contrast	0.797	0.652	0.856	0.556
Busyness	0	0.426	0	0.429
Percent change				
Conventional Indices				
SUV_{max}	-1.427	0.559	-22.688	0.475
SUV_{peak}	-15.454	0.625	9.566	0.468
TLG	-86.113	0.64	-86.113	0.493
CoV	-26.869	0.778	-26.869	0.558
MTV	-69.988	0.648	-78.286	0.51
Histogram Indices				
Skewness	-370.108	0.386	-348.952	0.507
Kurtosis	-25.780	0.487	14.883	0.423
Entropy $_{(log2)}$	-17.802	0.76	-13.379	0.556
Energy	234.991	0.317	4.415	0.472
Shape Indices				
Sphericity	-11.001	0.477	-6.102	0.417
Compacity	-37.465	0.705	-13.403	0.554
GLCM				
Contrast	-100	0.54	-3.631	0.538
Correlation	-100	0.449	-18.871	0.539
Entropy $_{(log2)}$	-26.118	0.861	-26.118	0.593
Dissimilarity	-21.951	0.742	-21.545	0.535
NGLDM				
Coarseness	-73.38	0.669	-43.184	0.54
Contrast	-15.94	0.559	-15.940	0.478
Busyness	-9.242	0.48	-25.591	0.492

ROC = receiver operating characteristics; AUC-ROC = area under the ROC curve; PFS = progression-free survival; OS = overall survival; SUV = standardized uptake values; Sd = standard deviation; TLG = total lesion glycolysis; CoV = coefficient of variation; MTV = metabolic tumor volume; GLCM = gray-level co-occurrence matrix; NGLDM = neighboring gray-level dependence matrix;

Supplemental Table 5. Univariate Cox regression analysis for PFS and OS

	PFS			OS		
	HR	95% CI	*P*	HR	95% CI	*P*
Clinical variables						
Age (≥60 vs. <60 (ref))	1.1	0.65-1.89	0.716	1.31	0.76-2.25	0.336
Gender (male vs. female (ref))	1.31	0.75-2.31	0.344	1.05	0.60-1.82	0.868
Initial disease status (metastatic vs. locally advanced (ref))	1.48	0.76-2.89	0.246	1.56	0.78-3.10	0.208
First-line chemotherapy regimen (FOLFIRINOX vs. gemcitabine-based (ref))	0.66	0.37-1.18	0.165	0.66	0.37-1.19	0.170
BMI (≥25 vs. 20-24.9 (ref))	1.08	0.57-2.03	0.807	0.78	0.34-1.76	0.546
BMI (<20 vs. 20-24.9 (ref))	0.44	0.18-1.05	0.062	1.46	0.72-2.55	0.342
DM (yes vs. no (ref))	0.84	0.46-1.55	0.578	1.1	0.62-1.96	0.749
Hypertension (yes vs. no (ref))	0.97	0.54-1.72	0.907	0.84	0.46-1.53	0.564
ECOG performance status (1-2 vs. 0 (ref))	0.98	0.56-1.72	0.942	1.16	0.66-2.03	0.606
CEA (≥10 vs. <10 (ref))	1.31	0.74-2.32	0.354	1.62	0.92-2.88	0.096
CA 19-9 (≥755 vs. <755 (ref))	1.86	1.08-3.19	0.024	1.81	1.05-3.11	0.031
Total bilirubin (≥1.3 vs. <1.3 (ref))	1.05	0.42-2.65	0.919	0.9	0.32-2.51	0.843
Albumin (<3.3 vs. ≥3.3 (ref))	1.81	0.77-4.26	0.176	2.15	0.90-5.13	0.084
Best response (non-responder vs. responder (ref))	1.91	1.03-3.54	0.039	1.42	0.77-2.59	0.258
T1 (baseline)						
Conventional Indices						
SUV_{max}		*Not included*[*]		1.53	0.87-2.67	0.138
SUV_{peak}	1.68	0.84-3.36	0.144	3.02	1.36-6.74	0.007
TLG	1.31	0.72-2.38	0.378	1.60	0.87-2.95	0.129
CoV		*Not included*		1.64	0.91-2.93	0.098
MTV	1.51	0.85-2.69	0.158	1.42	0.80-2.54	0.228
Histogram Indices						
Skewness	2.07	1.14-3.77	0.017		*Not included*	
Kurtosis	1.69	0.99-2.90	0.056	1.41	0.82-2.43	0.209
Entropy $_{(log2)}$		*Not included*		1.43	0.83-2.45	0.196
Shape Indices						
Sphericity	1.74	0.87-3.47	0.118		*Not included*	
Compacity	1.85	1.01-3.36	0.045	1.89	1.92-3.49	0.042
GLCM						
Dissimilarity		*Not included*		2.16	1.05-4.47	0.037
NGLDM						
Coarseness		*Not included*		1.68	0.93-3.04	0.087
T2 (first assessment)						

Conventional Indices						
SUV_{max}	2.16	1.18-3.97	0.013	2	1.10-3.65	0.024
SUV_{peak}	1.84	1.01-3.34	0.046		*Not included*	
TLG	1.5	0.86-2.61	0.149	2.18	1.21-3.92	0.01
CoV	2.57	1.38-4.78	0.003	2.52	1.32-4.79	0.005
MTV	1.75	0.99-3.10	0.053	1.61	0.90-2.86	0.108
Histogram Indices						
Kurtosis	1.8	0.98-3.31	0.059		*Not included*	
Entropy $_{(log2)}$	1.83	1.02-3.28	0.041	2.42	1.13-5.21	0.024
Shape Indices						
Sphericity	1.96	0.94-4.08	0.071		*Not included*	
Compacity	1.72	0.94-3.14	0.077	1.8	1.00-3.24	0.049
GLCM						
Entropy $_{(log2)}$	1.89	1.03-3.49	0.041	2.23	1.23-4.03	0.008
Dissimilarity	2.15	1.19-3.90	0.011	2.59	1.15-5.84	0.021
NGLDM						
Coarseness	1.54	0.87-2.73	0.141	2.43	1.24-4.79	0.01
Contrast	1.95	0.98-3.87	0.057		*Not included*	
Percentage changes						
Conventional Indices						
SUV_{peak}	2.04	1.13-3.68	0.018		*Not included*	
TLG	2.51	1.10-5.75	0.029		*Not included*	
CoV	3.79	1.81-7.92	<0.001		*Not included*	
MTV	1.64	0.86-3.11	0.131		*Not included*	
Histogram Indices						
Entropy $_{(log2)}$	2.2	1.19-4.06	0.011		*Not included*	
Shape Indices						
Compacity	1.64	0.86-3.12	0.132		*Not included*	
GLCM						
Entropy $_{(log2)}$	3.62	1.75-7.46	<0.001		*Not included*	
Dissimilarity	2.68	1.35-5.34	0.005		*Not included*	
NGLDM						
Coarseness	1.62	0.88-2.99	0.124		*Not included*	

PFS = progression-free survival; OS = overall survival; HR = hazard ratio; CI = confidence interval; FOLFIRINOX = folfirinic acid/fluorouracil/irinotecan/oxaliplatin; BMI = body-mass index; DM = diabetes mellitus; ECOG = Eastern Cooperative Oncology Group; CEA = Carcinoembryonic antigen; CA 19-9 = carbohydrate antigen 19-9; SUV = standardized uptake values; TLG = total lesion glycolysis; CoV = coefficient of variation; MTV = metabolic tumor volume; GLCM = gray-level co-occurrence matrix; NGLDM = neighboring gray-level dependence matrix;
*Variables with the area under the time-dependent receiver operating characteristics curve <0.6 were not included in the univariate analysis.